RESEARCH ARTICLE
doi: 10.2306/scienceasia1513-1874.2026.046

ScienceAsia 52 (3): 2026: ID 2026046: **1–9**

Characterization and evaluation of antioxidant and antifungal properties of a selenium-enriched lactic acid bacteria

Shize Liu[a,b,c], **Lingru Feng**[a,b,c], **Zijian Jiang**[a,b,c], **Siqi Huang**[a,b,c], **Yanfen Zheng**[a,b,c], **Jichang Yang**[d,*], **Huilin Yang**[a,b,c,*]

[a] College of Environment & Ecology, Hunan Agricultural University, Changsha, Hunan 410128 China
[b] Team of High Value Utilization of Crop Ecology, Yuelushan Laboratory, Changsha, Hunan 410128 China
[c] Hunan Provincial Key Laboratory of Rural Ecosystem Health in Dongting Lake Area, Changsha 410128 China
[d] Hunan Engineering Research Center of Internet-Chinese and Western Medicine Collaboration-Health Service, Hunan University of Medicine, Huaihua, Hunan 418000 China

*Corresponding authors, e-mail: yangjc1969@126.com, yanghuilin@hunau.edu.cn

Received 22 Oct 2025, Accepted 22 Apr 2026
Available online 29 May 2026

ABSTRACT: This study developed an environmentally friendly, selenium-enriched lactic acid bacteria (Se-LAB) preparation using *Lactobacillus delbrueckii* subsp. *bulgaricus* GIM1.155 to address selenium deficiency, oxidative stress-related diseases, and food safety. Optimal conditions (pH 6, 37 °C, 30 h, 3% (v/v) inoculation, 8 μg/ml ion concentration) achieved a 21.83 ± 0.69% inorganic selenium conversion rate. Selenium nanoparticles were 40–110 nm intracellularly and 100–340 nm extracellularly. The selenium-enriched *L. delbrueckii* subsp. *bulgaricus* GIM1.155 (Se-LBG) showed enhanced antioxidant properties and significant antifungal activity against *Aspergillus flavus* at 17 μg/ml, comparable to nystatin. This suggests its potential as a natural preservative, enhancing selenium bioavailability, antioxidant properties, and antifungal activity.

KEYWORDS: Se-enriched LAB, *Lactobacillus delbrueckii*, culture optimization, antioxidant, antifungal activity

INTRODUCTION

Lactic acid bacteria (LAB) effectively convert inorganic selenium into low-toxicity nano-selenium, enhancing their antioxidant properties [1]. The color of Se-LAB biomass indicates nano-selenium levels [2], and these enriched LAB have various applications in biological research [3]. Selecting suitable LAB strains is crucial for creating selenium-enriched products, focusing on their ability to convert selenium into absorbable forms and their health benefits, such as antioxidant and anti-inflammatory effects [4]. Optimizing the preparation process, including adjusting fermentation conditions like pH, temperature, and selenite concentration, is vital for improving production efficiency. For example, specific conditions increased selenium reduction efficiency in *Pediococcus acidilactici* DSM20284, *Lactobacillus bulgaricus*, and *Streptococcus thermophilus* to over 90% within 48 h [5].

In animal husbandry, Se-LAB are applied to elevate selenium content in animal products and ameliorate animal health. Dietary supplementation of Se-LAB in *Cyprinus carpio* has been shown to enhance growth performance, protect hepatic tissue, improve lipid metabolism, alleviate inflammation and boost antioxidant capacity, even under high-saline conditions [6]. In food fermentation, Se-enriched *Lactobacillus plantarum* (Se-enriched *L. plantarum*) improves the antioxidant activity, flavor and selenium content of fermented *Pleurotus eryngii*, accompanied by increased phenolic content and DPPH radical scavenging capacity [7]. The LAB also exert antifungal activity, which mitigates fungal toxin contamination and spoilage in fermented foods and agricultural products, thus reducing the associated hazards to humans and animals [7, 8]. Despite extensive research on Se-enriched LAB, studies specifically focusing on selenium enrichment in *Lactobacillus delbrueckii* subsp. *bulgaricus* (*L. delbrueckii* subsp. *bulgaricus*) remain limited. Yang et al [9] investigated the antibacterial activity of Se-enriched LAB, yet their work primarily analyzed fermentation broths and supernatants, with scarce attention to antifungal activity and dose-dependent antibacterial efficacy. Furthermore, existing antioxidant studies lack evaluations of the concentration-dependent antioxidant properties of Se-enriched LAB and the enhancements in antioxidant capacity induced by selenium enrichment [1].

Numerous studies have explored the preservative effects of supernatants and fermentation broths from Se-enriched LAB, but further research is required to evaluate their application as preservatives in agricultural products. Notably, *L. delbrueckii* subsp. *bulgaricus* is well recognized for its fermentation, probiotic, and antibacterial properties [10]. This study aimed to optimize and characterize the selenium enrichment of *L. delbrueckii* subsp. *bulgaricus*, evaluate its antifungal and antioxidant activities at different selenium concentrations, and assess its potential as an antifungal agent and antioxidant in agriculture and fermented foods.

MATERIALS AND METHODS

Strain and reagents

L. delbrueckii subsp. *bulgaricus* was obtained from the Guangdong Provincial Microbial Strain Collection Centre (GDMCC), Guangdong, China. *A. flavus* was preserved in the College of Environment and Ecology, Hunan Agricultural University, Changsha, China. 3,3′-Diaminobenzidine (DAB), 2,2-diphenyl-1-picrylhydrazyl (DPPH), 2,2′-azobis-3-ethylbenzothiazoline-6-sulphonic acid (ABTS), and Potato Dextrose Agar (PDA) were purchased from Beijing Coolaber Technology Co., Ltd., Beijing, China. All chemicals were of analytical grade (Shanghai Aladdin Biochemical Technology Co., Ltd., Shanghai, China) except nitric acid and hypochlorous acid (high purity). The Mann, Rogosa, Sharp (MRS) medium for LAB contained: casein peptone (10.0 g/l), beef extract (10.0 g/l), yeast extract (5.0 g/l), glucose (20.0 g/l), K_2HPO_4 (2.0 g/l), $MnSO_4 \cdot 7\,H_2O$ (0.05 g/l), $MgSO_4 \cdot 7\,H_2O$ (0.2 g/l), CH_3COONa (5.0 g/l), Tween 80 (1.0 g/l), and triammonium citrate (2.0 g/l), adjusted to pH 6.8. These chemicals were mixed under MRS formula.

Optimization of the preparation process for Se-LBG

L. delbrueckii subsp. *bulgaricus* was inoculated at 1% (v/v) into MRS medium (pH 6.8) containing different selenium concentrations (0, 2, 4, 6, 8, 10, 12, 14, 16 μg/ml). Fifty milliliters of the selenium-enriched MRS medium were incubated at 37 °C for 24 h. After incubation, 30 ml sterile saline was added to the bacterial pellets, vortexed, and centrifuged (4,000 rpm for 10 min). The supernatant was discarded, and the washing step was repeated 2–3 times. Each treatment was performed in triplicate, with results averaged to serve as a reference for subsequent orthogonal experiments [11].

We examined various culture conditions to identify key factors and minimize experimental effort. *L. delbrueckii* subsp. *bulgaricus* was grown in MRS medium (pH 6, 8 μg/ml selenium, 1% inoculum v/v) at temperatures from 29 °C, to 45 °C, for 24 h in a sealed environment. We then conducted single-factor experiments, altering one variable at a time (pH: 4–8; inoculum: 1–5%; selenium: 6–10 μg/ml; time: 6–30 h) while keeping others constant. Using Minitab 18, an L9(3^4) orthogonal design was applied (Table S1). Results indicated significant effects of pH, time, and temperature ($p < 0.05$), which were chosen for further testing, while inoculum (3%) and selenium concentration (8 μg/ml) were kept constant to explore optimal selenium transformation [11].

Selenium content determination in Se-LBG

Biomass determination, wet digestion pretreatment, and selenium content analysis of *L. delbrueckii* subsp. *bulgaricus* were performed using the DAB colorimetric method as per protocol [12]. The selenium standard curve was slightly modified from the method described [13]. Briefly, aliquots of a 15 μg/ml selenium standard solution (0 to 12 ml) were placed in 100 ml beakers, mixed with 35 ml ultrapure water, and processed as per the original method. Each assay included three biological replicates, with triplicates for each to determine the mean. Selenium cellular conversion rate and enrichment content were calculated using specific equations.

Cellular conversion rate (%) = (Total intracellular Se (μg)/Initial total added inorganic Se (μg)) × 100

Selenium enrichment content (%) = (Intracellular Se concentration (μg/ml) × Digestion solution volume (10 ml)/Bacterial cell biomass (g)) × 100

Characterization of Se-LBG

Under the optimal selenium-enrichment conditions, comprehensive characterization was conducted on Se-LBG. Se-LBG bacterial suspensions were analyzed for the size, morphology and distribution of selenium nanoparticles (Se-NPs) by biological transmission electron microscopy (TEM, Hitachi-7800, Hitachi, Japan). Fourier transform infrared spectroscopy (FT-IR, Nicolet iS50, Thermo Scientific, USA) was used to identify Se NP functional groups over a wavenumber range of 4000–400 cm^{-1}. Scanning electron microscopy (SEM) coupled with energy dispersive spectroscopy (EDS) (ZEISS Sigma 300, Germany) was employed to verify selenium accumulation in *L. delbrueckii* subsp. *bulgaricus*.

Detection of antioxidant activity in Se-LBG

The Se-LBG bacterial suspension was prepared with a selenium concentration of 23 μg/ml with a bacterial biomass concentration of 71.43 mg/ml. This suspension was subjected to 2-, 2.5-, 5-, and 10-fold serial dilution. The control group was non-selenium biomass with an initial bacterial biomass concentration of 71.43 mg/ml, which underwent the identical serial dilution to yield final concentrations ranging from 7.14 mg/ml to 71.43 mg/ml. The scavenging activities against DPPH radicals using DPPH-ethanol solution [6], hydroxyl radicals via the Fenton reaction, ABTS radicals with $ABTS^{\bullet+}$ solution, and reactive oxygen species (ROS) in Tris-HCl solution were determined following the methods described [13–15].

In vitro bacteriostatic activity of Se-LBG against *A. flavus*

The inhibitory effect of Se-LBG on *A. flavus* was evaluated via the growth rate method. Following optimal cultivation, Se-LBG was suspended in PBS and incorporated into PDA medium at three selenium concentrations (17, 8.5, and 4.25 μg/ml), corresponding

to bacterial biomass concentrations of 52, 26, and 13 mg/ml, respectively. The mixture was poured into 9 cm Petri dishes for solidification. A blank control (PBS only) and a positive control (Nystatin) were also prepared. Pre-cultured *A. flavus* on PDA was punched into 6 mm discs, which were placed with the mycelial side down at the center of each Petri dish. Each treatment was performed in triplicate, incubated inverted at 28 °C for 3 days. Mycelial growth inhibition rate was determined by the plate colony diameter method. After the control colonies formed typical circular morphology, colony diameters were measured via the cross method, and the mean values were substituted into the formula: inhibition rate = [(control colony diameter − treatment colony diameter)/control colony diameter] × 100%. Three replicates were performed for each group.

Effectiveness of Se-LBG on mold prevention in corn kernels

The inhibitory effect of Se-LBG on *A. flavus* was evaluated as described [13]. Healthy, undamaged corn kernels (moisture <13%) were selected and divided into three portions. After disinfection with 75% ethanol and thorough rinsing, samples were autoclaved at 121 °C for 30 min. Sterility was verified by PDA culture, aflatoxin B_1 was confirmed <0.1 µg/kg by ELISA, and the corn was stored at 4 °C. Each portion was sprayed with 3 ml of 17 µg/ml Se-LBG suspension. Nystatin was used as the positive control, and sterile water containing 0.5% Tween-80 as the blank control. Subsequently, 1×10^6 CFU/ml *A. flavus* spore suspension was uniformly sprayed onto the corn surface. Treated corn cubes were placed in sealed plastic boxes and incubated at 28 °C for 7 days. Disease occurrence assessment, grading criteria, disease index calculation, and relative control effect determination were performed as described by Cao et al [16].

Statistical analysis

Data were analyzed and plotted using SPSS 25 and GraphPad Prism 8. Analysis of variance (ANOVA) was employed to compare variable-treatment interactions. *p*-values were used to determine statistical significance. Orthogonal experimental design and analysis were performed using Minitab 18. All values are expressed as mean ± SD, with $p < 0.05$ considered statistically significant.

RESULTS

The selenium content standard curve, established via the DAB colorimetric method, is presented in Fig. S1. The curve is described by the equation $y = 0.8334x + 0.0137$, with a high coefficient of determination ($R^2 = 0.9991$), indicating excellent linear fitting and suitability for subsequent related analyses.

Effect of different culture conditions on the rate of selenium conversion

The optimal sodium selenite concentration was identified by measuring intracellular selenium and observing bacterial biomass color. Table S1 shows that selenium conversion rates in *L. delbrueckii* subsp. *bulgaricus* generally rose with higher selenium concentrations. At 8 µg/ml, the conversion rate was notably higher than at 4 and 6 µg/ml. The highest rate (19.73%) occurred at 14 µg/ml, but biomass was lower than at 8 µg/ml. Biomass dry weight decreased significantly as selenium concentration increased, especially beyond 8 µg/ml. The conversion rate at 14 µg/ml exceeded that at 16 µg/ml, resulting in a darker red color. Fig. 1 shows biomass was bright pink at 8 µg/ml; below this, it was mostly white with a pink tint, and above, it turned brick red. The optimal selenium concentration, based on biomass, selenium conversion rate, and color, is 8 µg/ml, yielding a conversion efficiency of 6.36 ± 0.18% and a biomass dry weight of 0.0466 ± 0.0008 g/50 ml.

The effects of five culture conditions (pH, temperature, inoculum volume, sodium selenite concentration, and time) on the selenium conversion rate and biomass of Se-LBG were investigated. Selenium conversion rate peaked at pH 6 and decreased at higher pH values, while biomass increased with rising pH and reached a maximum of 0.0406 ± 0.0019 g at pH 8. Both selenium conversion efficiency and biomass attained their maximum at 37 °C, with both indices declined at temperatures above this value. The highest selenium conversion rate (17.19 ± 2.69%) was observed at a 3% (v/v) inoculum volume, whereas biomass peaked at 4% inoculum volume. Selenium conversion rate reached its peak at 8 µg/ml sodium selenite (27.58 ± 1.94%), and biomass was the lowest at this concentration. Selenium conversion rate maximized at 24 h, while biomass reached a maximum of 0.0322 ± 0.0011 g at 30 h. Significance analysis revealed that initial pH, temperature and time significantly affected selenite transformation in *L. delbrueckii* subsp. *bulgaricus* ($p < 0.05$) (Fig. 2).

Orthogonal experiment design and analysis

The culture conditions were optimized via orthogonal experiments. Three key factors (pH, temperature, and time) were selected for optimization, and the fifth experimental set was found to yield the highest selenium conversion rate (Tables S2, S3). ANOVA demonstrated that all three factors significantly affected the selenium conversion rate, with the order of influence ranked as pH > temperature > stress time (Table 1). The predictive model derived from the orthogonal experiment identified the optimal conditions as follows: initial pH 6, temperature 37 °C, time 30 h, inoculum volume 3%, and sodium selenite concentration 8 µg/ml Validation experiments confirmed a selenium conversion rate

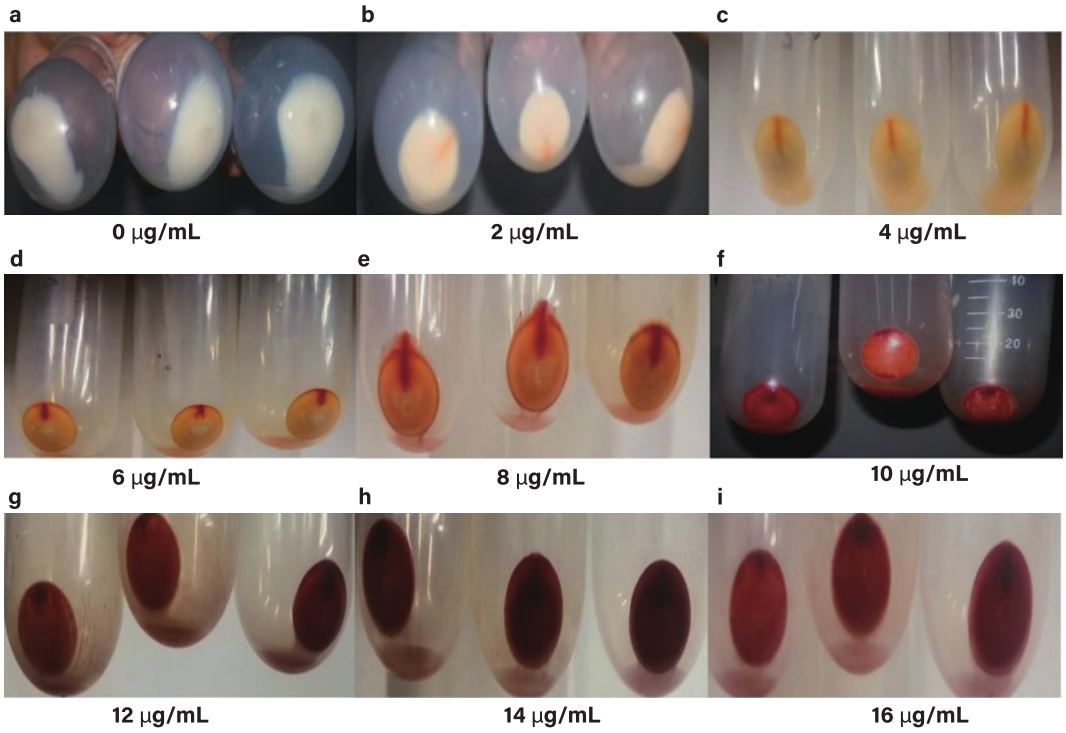

Fig. 1 The color of bacterial precipitation at selenium concentrations of 0, 2, 4, 6, 8, 10, 12, 14, and 16 μg/ml, respectively for a–i. (Pictures taken at the bottom of glass tubes, tube size is 15 mm × 150 mm in diameter)

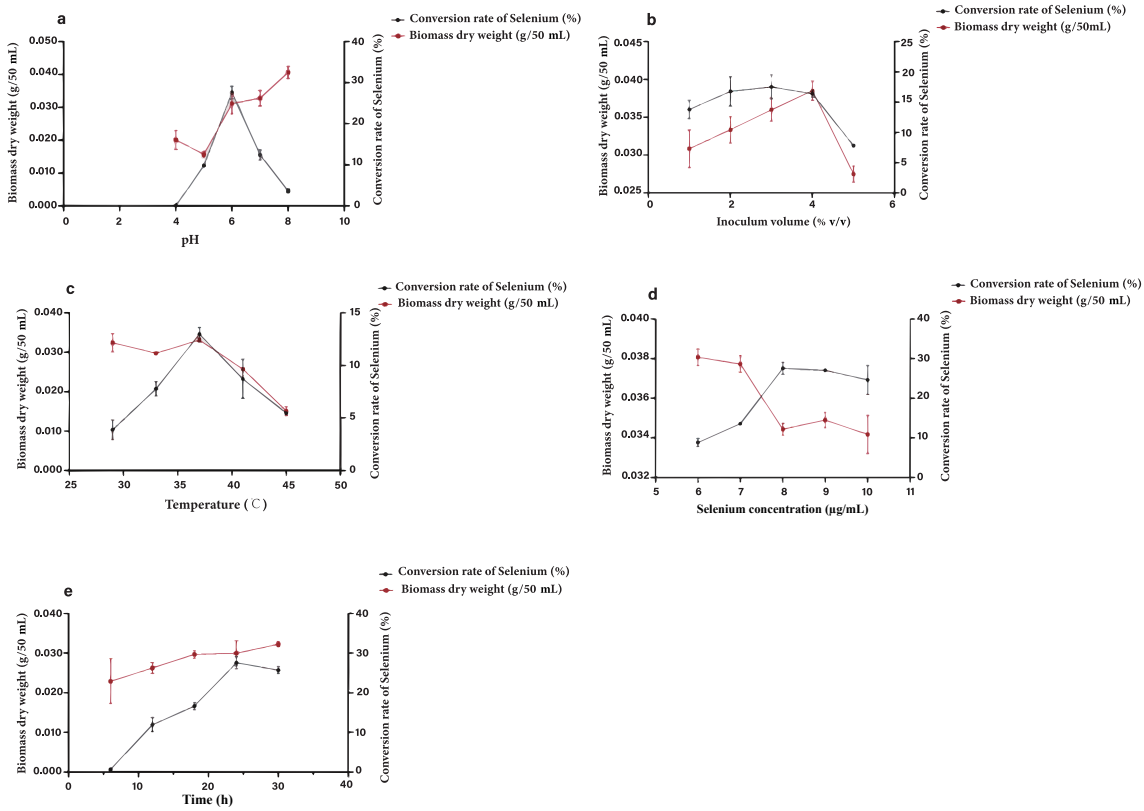

Fig. 2 Effects of various factors on selenium conversion rate and biomass. a: pH, b: inoculum volume, c: temperature, d: selenium concentration, e: time.

Table 1 Analysis of variance of orthogonal experiment results.

Source	Degree of freedom	Adj SS	Adj MS	*F* value	*p* value
Initial pH	2	93.873	46.9365	228.50	0.004*
Temperature (°C)	2	58.331	29.1657	141.99	0.007*
Time (h)	2	35.443	17.7217	86.27	0.011*
Error	2	0.411	0.2054		
Total	8	188.059			

Adj SS = Adjusted Sum of Squares; Adj MS = Adjusted Mean Square; * statistically significant.

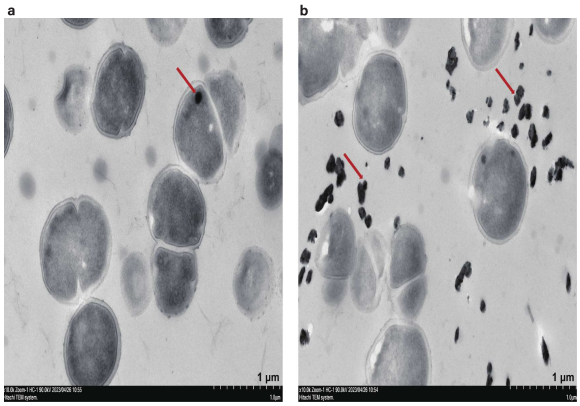

Fig. 3 TEM analysis results of Se-LBG. a: Intracellular presence of nano-selenium; b: Extracellular presence of nano-selenium; The arrow indicates selenium nanoparticles. The image size is 1 μm.

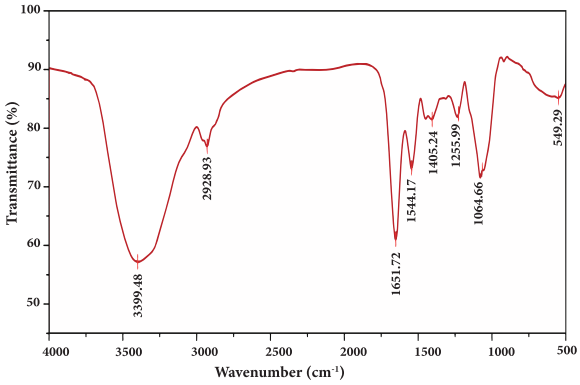

Fig. 4 FTIR spectroscopic characterization of Se-LBG cells.

of 21.83 ± 0.69% under these conditions, representing a relative increase of 15.47 ± 0.51%. These optimized culture conditions were subsequently adopted for the preparation of Se-LBG.

TEM and EDS analyses

After optimal cultivation, Se-LBG was washed, fixed with glutaraldehyde, and examined via TEM to study selenium enrichment and Se-NPs distribution in lactic acid bacteria. Fig. 3 shows Se-NPs localization, with particle sizes measured using Nano Measurer 1.2. Analysis of ten TEM images. The result revealed that intracellular Se-NPs were spherical (40–110 nm in size, averaging 66 nm) while extracellular Se-NPs were irregular (100–340 nm, averaging 190 nm). EDS analysis confirmed carbon (C), oxygen (O), sulfur (S), and selenium (Se) in the enriched bacterial products, as basic cellular components, consistent with microbial biomass (Fig. S2).

FTIR analysis

FTIR analysis was employed to characterize functional group variations in Se-LBG cells (Fig. 4). A strong and broad absorption band at 3397.15 cm^{-1} was assigned to O–H stretching vibrations, indicative of hydroxyl or phenolic groups. A weak band at 2929.99 cm^{-1} corresponded to saturated C–H stretching, confirming the presence of alkane (–CH_2–) and methylene moieties. The weak absorption at 1652.41 cm^{-1} suggested carbonyl-containing compounds. A moderate band at 1546.21 cm^{-1} arose from C=C or N–O stretching vibrations, implying nitro (NO_2) compounds. A weak broad doublet band at 1405.93 cm^{-1} was attributed to in-plane bending vibrations of saturated C–H bonds, supporting the presence of alkanes. Weak bands at 1235.33 cm^{-1} and 1079.03 cm^{-1} indicated the possible presence of alcohols, ethers, lipids, or amines.

Under optimal conditions, a Se-LBG suspension was prepared, using its non-selenium counterpart as the control. Linear regression analysis revealed that the antioxidant capacity of both suspensions increased with biomass concentration ($p < 0.001$) (Fig. 5). A paired t-test confirmed that the selenium-enriched group exhibited significantly stronger free radical scavenging activity than the control ($p < 0.001$), except for ABTS radicals. Compared with the non-selenium suspension, the selenium-enriched one showed enhanced antioxidant properties: at a selenium concentration of 2.3 μg/ml (corresponding to 7.14 mg/ml biomass), its scavenging efficiencies for DPPH, ABTS, and •OH radicals were increased by 2.47%, 11.68%, and 52.88%, respectively. At 9.2 μg/ml selenium (28.57 mg/ml biomass), ROS and •OH scavenging efficiencies were elevated by 22.40% and 26.72%, respectively. At 11.5 μg/ml selenium, the increases in •OH and ROS scavenging were 22.72% and 23.62%, respectively. At 23 μg/ml selenium, DPPH and ROS scavenging rates rose by 19.00% and 34.69%, respectively. These find-

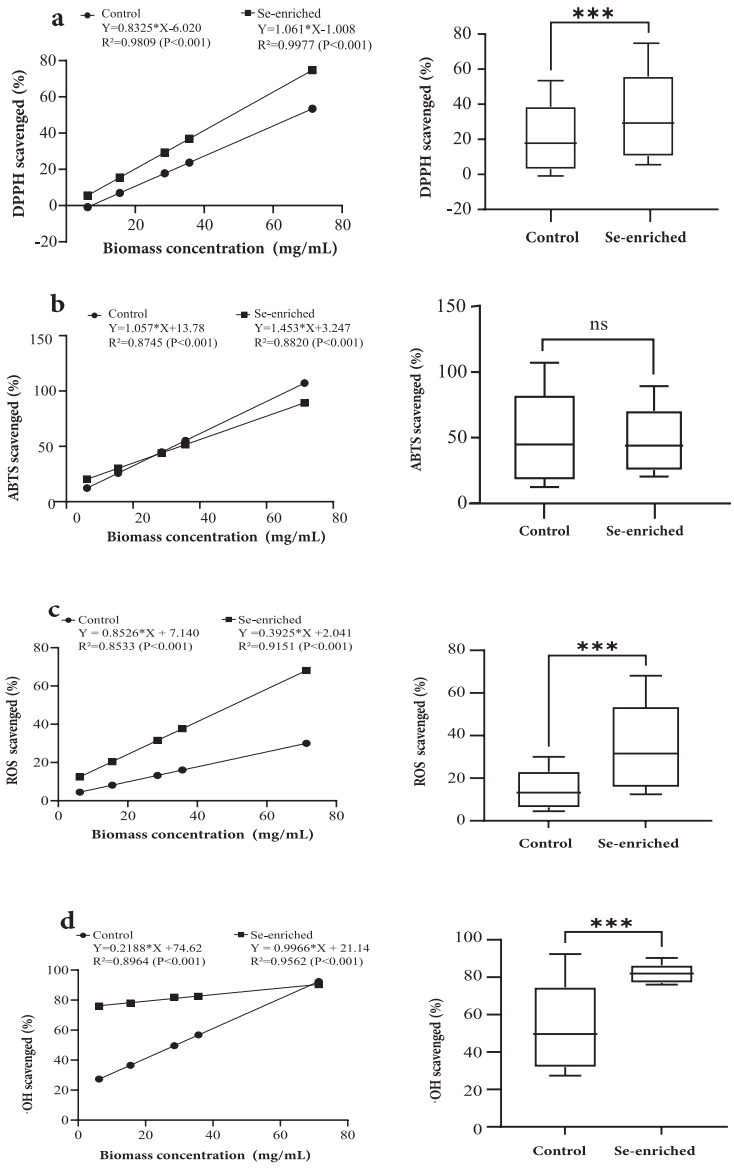

Fig. 5 Antioxidant activity of *L. delbrueckii* subsp. *bulgaricus* GIM1.155 and Se-LBG at different biomass concentrations: a: DPPH radical scavenging activity, b: ABTS radical scavenging activity, c: ROS radical scavenging activity, d: •OH radical scavenging activity. Statistical analysis: *** means $p < 0.001$, ns means no significant difference. Linear regression and paired T-test analyses were used.

ings indicated that the antioxidant performance of the Se-LBG suspension varied significantly with selenium concentration and free radical type, with particularly prominent effects on DPPH, ROS, and •OH scavenging.

In vitro antibacterial and antifungal effects of Se-LBG on corn kernels

Fig. 6 and Fig. 7 show that at 17 µg/ml selenium, Se-LBG inhibited *A. flavus* by 89.93 ± 0.74%. Nystatin's inhibition rates were 80.09 ± 1.06%, 89.24 ± 1.96%, and 91.20 ± 0.40% at 4.25, 8.5, and 17 µg/ml, respectively, with no significant difference from Se-LBG at 17 µg/ml. This concentration was used for further corn mold control tests. Fig. 7 indicates no mold growth in any group for the first 5 days. By day 7, *A. flavus* appeared on control samples but not in natamycin or Se-LBG groups. Using a sensitive corn mold index (Table S4), the control had 55.56% fungal contamination, while both treatments achieved 100% inhibition, showing Se-LBG's antifungal activity matches that of natamycin at the same concentration.

DISCUSSION

Optimizing culture conditions is critical for maximizing selenium conversion efficiency and biomass of the target strain [17]. Optimal pH and selenium

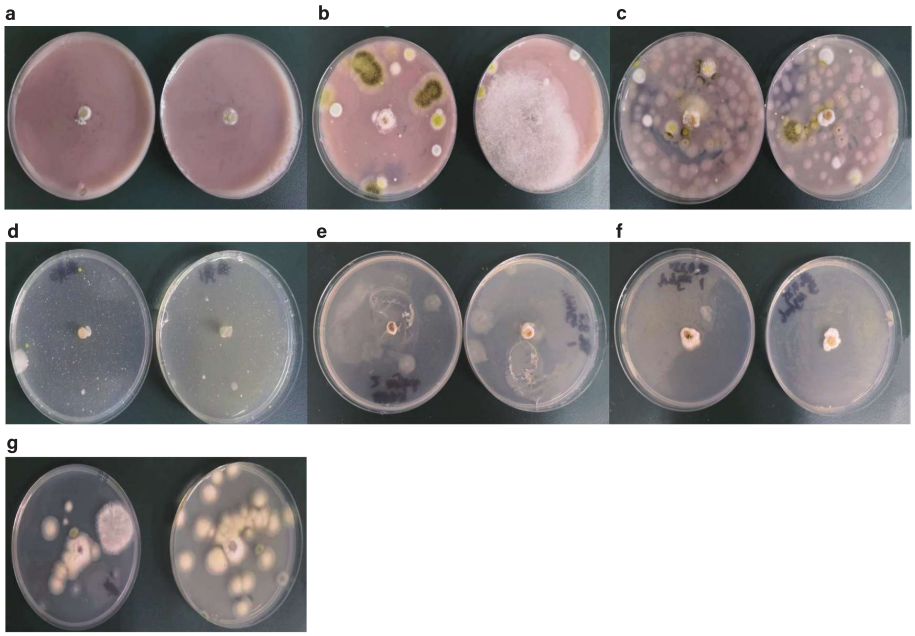

Fig. 6 Inhibition of *A. flavus* growth by Se-LBG and nystatin. a–c: Se-LBG at 17, 8.5, and 4.25 μg/ml, respectively. d–f: Nystatin at 17, 8.5, and 4.25 μg/ml, respectively. g: Control group.

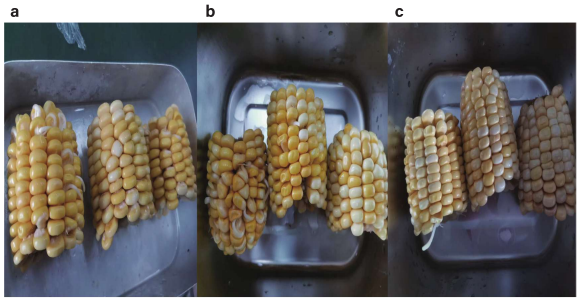

Fig. 7 The effects of a: control group, b: antibiotic group, and c: Se-LBG group on *A. flavus*-infected corn. The concentrations of nystatin and selenium rich groups were both at 17 μg/ml.

concentrations differ by species, influencing selenium conversion and biomass [18]. This study showed that higher pH and selenium levels decrease selenium conversion and biomass, aligning with previous findings that high pH (>6) or Na_2SeO_3 (>4.0 mM) reduced LAB-SeNPs' selenium conversion efficiency [19]. High selenium concentrations are toxic, lowering cellular biomass and microbial selenium reduction [20]. Moreover, selenium-enriched LAB can harm host intestinal microbiota at doses over 3.0 mg Se/kg, indicating toxicity at high levels [18]. Although 6 μg/ml is the reported optimal selenium concentration for LAB [14], our study showed 8 μg/ml induced *L. delbrueckii* subsp. *bulgaricus*'s pink pigmentation which meets production requirements. The maximum selenium conversion at 24 h fermentation, unlike *Lactobacillus paracasei* (peak at 32 h) [19]. The optimal temperature for growth and selenite biotransformation was 37 °C [5], with an optimal inoculum of 3% (v/v) differing from the reported 6% for *L. bulgaricus* and *S. thermophilus*, and 1% for *L. plantarum* and *Lactobacillus reuteri*, likely due to nutrient depletion at high inoculum and delayed growth at low inoculum [21]. Under optimized conditions (pH 6, 37 °C, 30 h fermentation, 3% (v/v) inoculum, 8 μg/ml selenium), the selenium conversion rate reached 21.83% ± 0.69% in this study which was lower than values from other LAB (e.g., 65.35% from *Lactobacillus rhamnosus* ATCC 53103 using response surface methodology [22]. LAB selenite reduction and biotransformation depend on strain-specific metabolic capacity, environmental adaptability, and genetic determinants of selenium transport/reductase systems [23]. For example, *Lactobacillus casei* ATCC 393 upregulates selenium metabolism-associated proteins during logarithmic growth [24]. Low selenite promotes growth/biotransformation, while high concentrations induce detoxification and reduce biomass [25]. Thus, the relatively low conversion rate is speculated to result from insufficient selenium metabolism genetic potential and selenite biotoxicity [26].

Intracellular SeNP biosynthesis involves direct synthesis and intermediates like selenodiglutathione [27]. FTIR spectroscopy highlights hydroxyl and phenolic groups as crucial for LAB-mediated SeNP biosynthesis [19]. Hydroxyl groups help maintain cell structure and bind Se(IV) [19], enhancing SeNP stability and uniformity. EDS and FTIR analyses show strains like *L. rhamnosus* ATCC 53103, *Enterococcus durans*

EF8-1 [28], and *Escherichia coli* DSM 20284 [4] encapsulate SeNPs with polysaccharides and proteins. Phenolic groups protect LAB from selenium-induced oxidative stress through antioxidant and Se(IV)-chelating actions [7]. TEM reveals that extracellular SeNPs have irregular shapes and larger sizes due to low phenolic content. EDS analysis confirms the presence of C, O, S, and Se, underscoring these groups' roles in SeNPs formation [9].

Balancing cost-effectiveness, stability, and consumer acceptability is crucial for the practical use of low-dose Se-LAB, which offers significant advantages. At 4 µg/ml sodium selenite, *L. plantarum* produces antioxidant metabolites to degrade nitrite [29]. Our study revealed that Se-LBG has a free radical scavenging capacity of 60%–90%. Selenium biotransformation in these preparations creates highly bioactive selenium species, enhancing antioxidant capacity through both enzymatic and non-enzymatic mechanisms [30], unlike conventional LAB. Selenium-amino acid compounds are highly water-soluble, thermally stable, and 85%–95% bioavailable. They are incorporated into GSH-Peroxidase and Thioredoxin Reductase, which scavenge H_2O_2 and lipid peroxides through enzymatic reactions, disrupting free radical chain reactions [17]. Se-NPs, with favorable colloidal stability, large specific surface area, and abundant surface electrons, scavenge free radicals through direct electron transfer, surface adsorption, and catalytic ROS dismutation [31]. Both can activate the transcription factor Nrf2 and upregulate *HO-1* and *NQO-1* gene expression [32].

The development of eco-friendly antifungal agents is driven by antibiotic resistance and environmental concerns. Here, Se-LBG suspension inhibited ∼90% of *A. flavus* at a low dose, showing strong antifungal effects. The Se-LAB's activity is primarily due to SeNPs, which cause physical damage, enhance antimicrobial metabolite secretion, inhibit enzymes, disrupt oxidative stress, and compete with pathogens [26, 27]. Selenium-free bacteria have normal cell structures, while selenium supplementation results in small spherical particles forming on and around cells [23]. Both intracellular and extracellular SeNPs were found in Se-LAB, indicating that its antifungal effectiveness is due to Se-LAB-derived antimicrobial substances and SeNP-induced damage. SeNPs' nanoscale size and large surface area disrupt fungal spore enzymes and proteins [33], as shown from the report on *L. paracasei* SeNPs inhibiting Candida/Fusarium and damaging Fusarium hyphae [22]. Key LAB pathways enhance secretion of organic acids, bacteriocins, and volatile compounds [33]. Selenium-enriched *L. plantarum* showed strong anti-*C. albicans* activity, likely due to selenium dioxide-induced antimicrobial metabolites [34]. *L. rhamnosus* also combats *C. albicans* by competing for nutrients and altering the growth environment [35]. Understanding differences between selenium-free and selenium-enriched LAB is crucial. Future research should employ multi-omics and *in vitro*/*in vivo* methods to study antibacterial activity and synergy.

CONCLUSION

This study developed a Se-LBG formulation with a 21.83% selenium conversion rate, exhibiting significant antioxidant and antifungal activities. At 17 µg/ml Se, the formulation inhibited *A. flavus* by 90% and corn spoilage by 100%, comparable to antibiotics. Additionally, the work enriched the characterization of Se-LBG. However, detailed mechanisms of selenium enrichment, antioxidant and antifungal activities require further investigation, as do their broader applications in other fields. In summary, this study provides valuable insights for the application of Se-LBG in agriculture, food safety, and fermentation.

Appendix A. Supplementary data

Supplementary data associated with this article can be found at https://dx.doi.org/10.2306/scienceasia1513-1874.2026.046.

Acknowledgements: This work was supported by Scientific Research Fund of Hunan Provincial Education Department (Nos. 20A254).

REFERENCES

1. Krausova G, Kana A, Hyrslova I, Mrvikova I, Kavkova M (2020) Development of selenized lactic acid bacteria and their selenium bioaccummulation capacity. *Fermentation* **6**, 13.
2. Saini K, Tomar SK, Sangwan V, Bhushan B (2014) Evaluation of Lactobacilli from human sources for uptake and accumulation of selenium. *Biol Trace Elem Res* **160**, 433–436.
3. Norouzi S, Daneshyar M, Farhoomand P, Tukmechi A, Tellez-Isaiasc G (2023) *In vitro* evaluation of probiotic properties and selenium bioaccumulation of lactic acid bacteria isolated from poultry gastrointestinal, as an organic selenium source. *Res Vet Sci* **162**, 104934.
4. Wang Q, Wang C, Kuang S, Wang D, Shi Y (2023) Biological selenite reduction, characterization and bioactivities of selenium nanoparticles biosynthesised by *Pediococcus acidilactici* DSM2028 4. *Molecules* **28**, 3793.
5. Yang J, Li Y, Zhang L, Fan M, Wei X (2017) Response surface design for accumulation of selenium by different lactic acid bacteria. *3 Biotech* **7**, 52.
6. Che X, Geng L, Zhang Q, Wei H, He H, Xu W, Shang X (2024) Selenium-rich *Lactobacillus plantarum* alleviates salinity stress in *Cyprinus carpio*: growth performance, oxidative stress, and immune and inflammatory responses. *Aquacult Rep* **36**, 102058.
7. Wang BY, Zhao N, Li J, Xu RY, Wang TR, Guo L, Ma M, Fan MT, et al (2021) Selenium-enriched *Lactobacillus plantarum* improves the antioxidant activity and flavor properties of fermented *Pleurotus eryngii*. *Food Chem* **345**, 128770.
8. Hymery N, Vasseur V, Coton M, Mounier J, Jany J, Barbier G, Coton E (2014) Filamentous fungi and mycotoxins in cheese: A review. *Compr Rev Food Sci F* **13**, 437–456.

9. Yang J, Wang J, Yang K, Liu M, Qi Y, Zhang T, Fan M, Wei X (2018) Antibacterial activity of selenium-enriched lactic acid bacteria against common food-borne pathogens *in vitro*. *J Dairy Sci* **101**, 1930–1942.
10. Song J, Zhou J, Li X, Li P, Tian G, Zhang C, Zhou D (2022) Nano-selenium stablilized by konjac glucommannan and its biological activity *in vitro*. *LWT* **161**, 113289.
11. Sun Y, Wang H, Zhou L, Chang M, Yue T, Yuan Y, Shi Y (2022) Distribution characteristics of organic selenium in Se-enriched *Lactobacillus* (*Lactobacillus paracasei*). *LWT* **165**, 113699.
12. Zeng Y, Guo X, Zhou K, Liu S, Han X (2015) Screening and Identification of Se-enriching lactic acid bacteria. *Food Sci* **36**, 178–182. [in Chinese with English summary]
13. Fang J, Lu J, Zhang Y, Wang J, Wang S, Fan H, Zhang J, Dai W, et al (2021) Structural properties, antioxidant and immune activities of low molecular weight peptides from soybean dregs (Okara). *Food Chem X* **12**, 100175.
14. Złotek U, Michalak-Majewska M, Szymanowska U (2016) Effect of jasmonic acid elicitation on the yield, chemical composition, and antioxidant and anti-inflammatory properties of essential oil of lettuce leaf basil (*Ocimum basilicum* L.). *Food Chem* **213**, 1–7.
15. Yu HS, Jang HJ, Lee NK, Paik HD (2019) Evaluation of the probiotic characteristics and prophylactic potential of *Weissella cibaria* strains isolated from kimchi. *LWT* **112**, 108229.
16. Cao S, Jiang B, Yang G, Pan G, Pan Y, Chen F, Gao Z, Dai Y (2023) Isolation and evaluation of *Bacillus subtilis* RSS-1 as a potential biocontrol agent against *Sclerotinia sclerotiorum* on oilseed rape. *Eur J Plant Pathol* **166**, 9–25.
17. Liao JJ, Wang CH (2022) Factors affecting selenium-enrichment efficiency, metabolic mechanisms and physiological functions of selenium-enriched lactic acid bacteria. *J Future Foods* **2**, 285–293.
18. Zhou J, Obianwuna UE, Zhang L, Liu Y, Zhang H, Qiu K, Wang J, Qi G, et al (2025) Comparative effects of selenium-enriched lactobacilli and selenium-enriched yeast on performance, egg selenium enrichment, antioxidant capacity, and ileal microbiota in laying hens. *J Anim Sci Biotechnol* **16**, 27.
19. El-Saadony MT, Saad AM, Taha TF, Najjar AA, Zabermawi NM, Nader MM, AbuQamar SF, ElTarabily KA, et al (2021) Selenium nanoparticles from *Lactobacillus paracasei* HM1 capable of antagonizing animal pathogenic fungi as a new source from human breast milk. *Saudi J Biol Sci* **28**, 6782–6794.
20. Zhang YZ, Wang BY, Zeng ZA, Xu RY, Li J, Fan MT, Wei XY (2020) Effect of culture conditions on the formation of selenium nanoparticles with different particle sizes by microbial reduction using *Lactobacillus plantarum* and their bioactivity evaluation. *Food Sci* **41**, 119–126. [in Chinese with English abstract]
21. Alzate A, Pérez-Conde M C, Gutiérrez A M, Cámara C (2010) Selenium-enriched fermented milk: A suitable dairy product to improve selenium intake in humans. *Int Dairy J* **20**, 761–769.
22. Xu Y, Wu S, He J, He C, Wang P, Zeng Q, Yang F (2020) Salt-induced osmotic stress stimulates selenium biotransformation in *Lactobacillus rhamnosus* ATCC 53103. *LWT* **131**, 109763.
23. Chen J, Jia Y, Chensheng H, Feng L, Li Y, Jian T, Han X, Niu X, et al (2025) Study on the probiotic properties of Xinjiang-characteristic selenium-enriched lactic acid bacteria and the distribution of selenium element. *Foods* **14**, 3577.
24. Martínez FG, Moreno-Martin G, Pescuma M, Madrid-Albarrán Y, Mozzi F (2020) Biotransformation of selenium by lactic acid bacteria: formation of seleno-nanoparticles and seleno-amino acids. *Front Bioeng Biotech* **8**, 506.
25. Kousha M, Yeganeh S, Keramat, Amirkolaie A (2017) Effect of sodium selenite on the bacteria growth, selenium accumulation, and selenium biotransformation in *Pediococcus acidilactici*. *Food Sci Biotechnol* **26**, 1013–1018.
26. Zhou M, Wang Q, Yang R (2024) Comparative study on growth and metabolomic profiles of six lactobacilli strains by sodium selenite. *Microorganisms* **12**, 1937.
27. Ranjard L, Prigent-Combaret C, Favre-Bonté S, Monnez C, Nazaret S, Cournoyer B (2004) Characterization of a novel selenium methyltransferase from freshwater bacteria showing strong similarities with the calicheamicin methyltransferase. *Biochim Biophys Acta Gene Struct Expr* **1679**, 80–85.
28. Liu J, Shi L, Tuo X, Ma X, Hou X, Jiang S, Lv J, Cheng Y, et al (2022) Preparation, characteristic and anti-inflammatory effect of selenium nanoparticle-enriched probiotic strain *Enterococcus durans* A8-1. *J Trace E Med Bio* **74**, 127056.
29. Zhang Y, Roh YJ, Han SJ, Park I, Lee HM, Ok YS, Lee BC, Lee SR (2020) Role of selenoproteins in redox regulation of signaling and the antioxidant system: A review. *Antioxidants* **9**, 383.
30. Chen Y, Li Q, Xia C, Yang F, Xu N, Wu Q, Hu Y, Xia L, et al (2019) Effect of selenium supplements on the antioxidant activity and nitrite degradation of lactic acid bacteria. *World J Microbiol Biotechnol* **35**, 61.
31. Jagoda Szafrańska, Małgorzata Ziarno, Marek Kieliszek (2025) Characterization of selenium accumulation in *Lactiplantibacillus plantarum* strains: A biotechnological approach. *Int J Vitam Nutr Res* **95**, 44231.
32. Ullah A, Mu J, Wang F, Chan MWH, Yin X, Liao Y, Mirani ZA, Sebt-E-Hassan S, et al (2022) Biogenic selenium nanoparticles and their anticancer effects pertaining to probiotic bacteria: A review. *Antioxidants (Basel)* **11**, 1916.
33. Xu C, Qiao L, Ma L, Guo Y, Dou X, Yan S (2019) Biogenic selenium nanoparticles synthesized by *Lactobacillus casei* ATCC 393 alleviate intestinal epithelial barrier dysfunction caused by oxidative stress via nrf2 signaling-mediated mitochondrial pathway. *Int J Nanomed* **14**, 4491–4502.
34. Liu J, Zhu X, Chen X, Liu Y, Gong Y, Yuan G, Liu J, Chen L (2020) Defense and inhibition integrate dmesoporous nanoselenium delivery system against tomato gray mold. *Environ Sci Nano* **7**, 210–227.
35. Kheradmand E, Rafii F, Yazdi MH, Sepahi AA, Shahverdi AR, Oveisi MR (2014 The antimicrobial effects of selenium nanoparticle-enriched probiotics and their fermented broth against *Candida albicans*. *Daru 6* **22**, 48.

Appendix A. Supplementary data

Table S1 Changes in biomass dry weight and conversion rate of selenium at different selenium concentrations. Different letters represent statistically significant differences within the same group ($p < 0.05$).

Selenium concentration (μg/ml)	Selenium conversion rate (%)	Biomass dry weight (g/50 ml)
2	6.17 ± 0.71^{d}	0.0475 ± 0.0006^{a}
4	3.27 ± 0.26^{e}	0.0475 ± 0.0008^{a}
6	5.82 ± 0.98^{d}	0.0466 ± 0.0008^{ab}
8	6.36 ± 0.18^{d}	0.0456 ± 0.0004^{c}
10	10.86 ± 0.24^{c}	0.0422 ± 0.0009^{c}
12	16.33 ± 0.37^{bc}	0.0393 ± 0.0010^{d}
14	19.73 ± 1.77^{a}	0.0351 ± 0.0002^{e}
16	17.53 ± 2.10^{ab}	0.0343 ± 0.0001^{e}

Table S2 Orthogonal test factors and levels.

Level	Initial pH	Temperature (°C)	Time (h)
1	5	33	18
2	6	37	24
3	7	41	30

Table S3 Orthogonal experiment results.

Exp. No	Initial pH	Temperature (°C)	Time (h)	Conversion of selenium (%)
1	5	33	18	5.85
2	5	37	24	13.43
3	5	41	30	14.99
4	6	33	24	11.63
5	6	37	30	21.16
6	6	41	18	15.45
7	7	33	30	7.74
8	7	37	18	8.58
9	7	41	24	8.32
K1	11.423	8.407	9.960	
K2	16.080	14.390	11.127	
K3	8.213	12.920	14.630	
R	7.867	5.983	4.670	
Factor order	1	2	3	

Table S4 Effectiveness of different drug concentrations against mold in corn kernels on day 7.

	Se-LBG group	Antibiotic group	Control group
Corn mold index	–	–	55.56%
Control effect	100%	100%	–

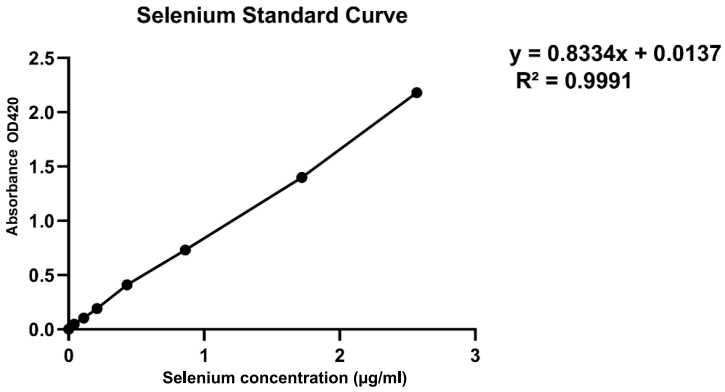

Fig. S1 The standard curve of selenium.

Element	Weight %	Atomic %	Error %	Net Int.	K Ratio	Z	A	F
C K	63.13	74.41	6.52	12413.88	0.3687	1.0509	0.5558	1.0000
O K	25.85	22.88	9.05	3764.00	0.0922	0.9927	0.3595	1.0000
Se L	8.23	1.47	3.31	1187.25	0.0551	0.6515	1.0274	1.0000
S K	2.80	1.24	5.38	473.08	0.0235	0.8569	0.9770	1.0051

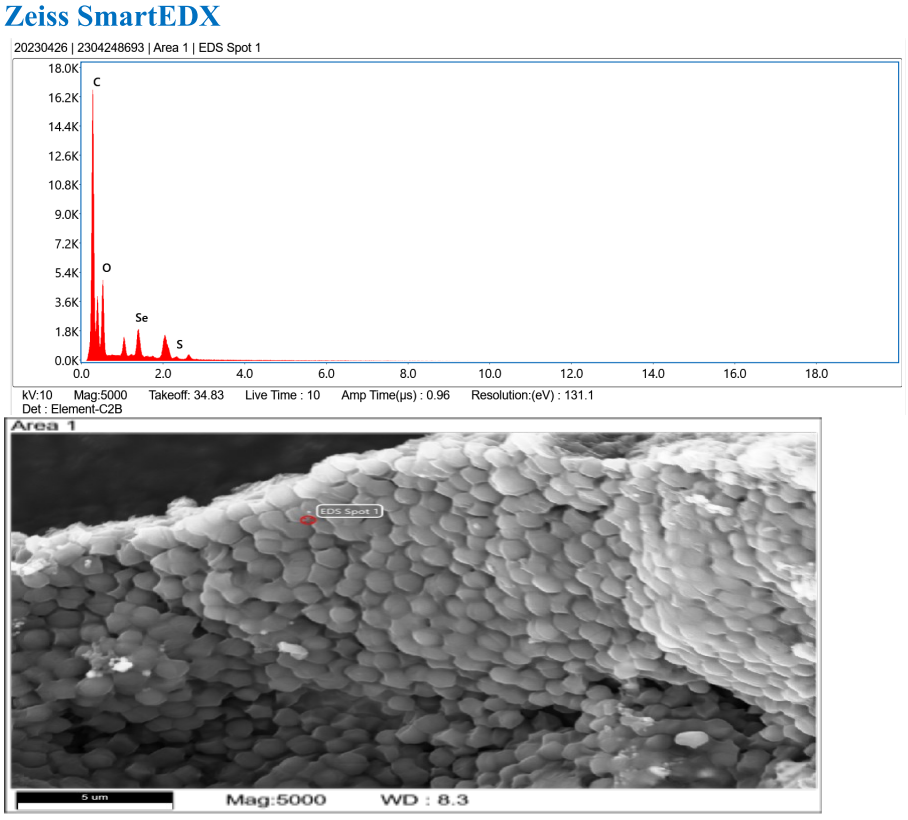

Fig. S2 The results of EDS analysis.